공학석사학위논문

Simple synthesis of CuO/Ag nanocomposite electrode using precursor ink for non-enzymatic electrochemical hydrogen peroxide sensing

전구체 잉크를 통해 산화구리/은 복합체로 제조된 전극 개발

및 과산화 수소의 비효소 전기화학적 검출

2018 년 2 월

서울대학교 유합과학기술대학원

융합과학부 나노융합전공

Wytse Hooch Antink

Simple synthesis of CuO/Ag nanocomposite electrode using precursor ink for non-enzymatic electrochemical hydrogen peroxide sensing

지도 교수 박원철

이 논문을 공학석사 학위 논문으로 제출함

2018 년 2 월

서울대학교 융합과학기술대학원

융합과학부 나노융합전공

Wytse Hooch Antink

Wytse Hooch Antink의 석사학위논문을 인준함

2017 년 12월

위 원 장 김연상 (인)

부 위 원 장 박원철 (인)

위 원 송윤규 (인)

Simple synthesis of CuO/Ag nanocomposite electrode using precursor ink for non-enzymatic electrochemical hydrogen peroxide sensing

Wytse Hooch Antink

Program in Nano Science and technology

Graduate School of Convergence Science & Technology

Seoul National University

Abstract

Hydrogen peroxide (H_2O_2) is an integral part in many biological processes, and is often used in industry as oxidizing agent for bleaching pulp or paper, as disinfectant for wastewater treatment and can even be found in some cosmetics, such as hair bleaching or teeth whitening. Although applying low concentrations of H_2O_2 may potential help disinfect wounds, exposure of the skin or eyes to higher concentrations of H_2O_2 are hazardous and possibly carcinogenic. The United States National Institute for Occupational Safety and Health classifies exposure to concentrations above 75 ppm as immediately dangerous to life or health. The detection of H_2O_2 is therefore vital and has traditionally been done through methods such as titrimetry, spectrophotometry and chemiluminescence. However, since these methods are time-consuming and complicated, electrochemical detection has become the preferred method of detection. Enzyme based sensors display good performance and selectivity but struggle with stability issues and high cost, leading most recent research to be focused on nanomaterial based sensors.

Herein we report a simple preparation method for a CuO/Ag composite electrode using precursor type ink without the need of a reducing

atmosphere or high temperatures. Thermogravimetric analysis (TGA) showed that the precursor type ink completely decomposes when heated at 150 °C and Scanning Electron Microscopy revealed a connective network of particles around 250 nm in size. The electrodes were used to make an amperometric sensor and electrochemical analysis showed that the sensor had a linear response in a wide range (5-500 μM) and a low detection limit of 4.0 μM (S/N=3). Compared to the pure silver electrode, the addition of the copper precursor to the silver ink resulted in a significant improvement in the limit of detection of H_2O_2.

Keywords: **CuO/Ag composite, Metal-organic decomposition ink, Non-enzymatic sensor, Hydrogen peroxide**

Student Number: **2015-26112**

Contents

List of Figures

List of Tables

1. Introduction

Despite its simple chemical structure, hydrogen peroxide (H_2O_2) can be found in many biological processes and in a multitude of different sectors in industry. In living organisms, H_2O_2 plays a vital role as signaling molecule in regulating processes such as immune cell activation and apoptosis, and is the side product of biochemical reactions of many common enzymes such as glucose oxidase (GOx), alcohol oxidase (ALOx), Cholesterol oxidase (ChoOx), etc [1]. In industry, H_2O_2 can have a variety of functions such as oxidizing agent for bleaching pulp and paper, disinfectant for wastewater treatment or even is the main component in many teeth whitening and hair bleaching cosmetics [2–4]. However, despite its many useful applications, working with H_2O_2 is not without any danger and according to the United States National Institute for Occupational Safety and Health, exposure to concentrations above 75 ppm classifies as immediately dangerous to life or health. Research into accurate and precise H_2O_2 sensors is thus not only interesting from an academic standpoint but is also of significant importance to many fields in industry.

Traditional detection techniques for H_2O_2 such as titrimetry [5,6], spectrophotometry [7,8] and chemiluminescence [9,10], chromatography [11], fluorescence [12] and phosphorescene [13] all suffer from one or several drawbacks such as high cost, low sensitivity and selectivity, are time-consuming or are susceptibility to interference.

Electrochemical sensors have reliably shown high sensitivity and selectivity, fast response time, simplicity and cost-efficiency and has thus become the preferred methods for H_2O_2 detection [14,15]. Especially redox protein based biosensors incorporating heme proteins like horseradish peroxidase (HRP), hemoglobin (Hb), myglobin (Mb) etc., have shown remarkable sensitivity but have some fundamental flaws such as the need for immobilization, poor stability, low reproducibility and the high cost of the enzymes [16–18].

1.1 Non-Enzymatic Sensor

Due to the rapid improvement in nanoscience and technology, sensors using metallic nanoparticles have become an attractive alternative to enzyme-based sensors. Especially the high surface-to-volume ratio of these metallic nanoparticles makes them ideal for catalytic purposes while minimizing the use of expensive metals. A wide variety of metals such as Pd [19], Pt [20] and Cu [21], and metal oxides such as NiO [22], Co_3O_4 [23] and Fe_3O_4 [24] have been suggested and studied as possible electrocatalysts.

Silver nanoparticles form an attractive non-enzymatic alternative due to their high conductivity and unique electronic properties [25,26]. Hydrothermal synthesis is the most common technique for the preparation of Ag nanoparticles, which provides monodisperse nanoparticles with good

control over shape and size. For example, Lu et al. [27] reported the synthesis of stable 5 nm Ag nanoparticles using an aqueous $AgNO_3$ solution and poly[(2-ethyldimethylammonioethyl methacrylate ethyl sulfate)-co-(1-vinylpyrrolidone)] (PQ11), without the need for any reducing agent or protecting agent. The resulting amperometric sensor displayed a linear range from 1×10^{-4} M to 0.18 M ($r = 0.998$) and a detection limit of 3.39×10^{-5} M (S/N=3).

Copper nanoparticles have been successfully synthesized through a variety of different methods, but their practical implementation is often hindered since they are well known to be unstable and susceptible to oxidation. However, copper oxide nanoparticles are considerably more stable and have been used in a variety of different applications, including electrochemical sensors. Using a chemical reduction method, Liu et al. [28] synthesized Cu_2O nanocubes wrapped by graphene (Cu_2O/GNs). The Cu_2O/GNs modified electrodes were used to make an amperometric sensor to detect both H_2O_2 and glucose and showed a limit of detection of 20.8 μM and 3.3 μM respectively.

It is well know that the combination of different metals and/or metal-oxides can lead to synergistic effects and enhanced performance compared to their individual components [29–31]. In particular, Cu-Ag composite materials have displayed excellent electrocatalytic performance in the detection of several different molecules such as H_2O_2 [32,33], glucose [34],

nitrite [35] and 2-butanone [36]. However, the need for a reducing atmosphere increases production cost and high sintering temperatures makes it impossible to use most plastic substrates, limiting the possible applications of Cu-Ag composites [37,38]. Lately Cu_2O/Ag composites have also been reported to possess excellent electrocatalytic performance as a H_2O_2 sensor without the need for a reducing atmosphere during the synthesis process [39,40].

1.2 Conductive Ink

Recently conductive inks and printed electronics have gained considerable attention. Compared to traditional methods such as photolithography, printing techniques allow for fast and low-cost fabrication of circuits and electrodes [41,42]. Different materials can be used to make conductive inks such as nanoparticles, organometallic complexes, conductive polymers, graphene oxide or carbon nanotubes. Nanoparticle based conductive inks are the most common and consist of a suspension of nanoparticles in a solvent that readily evaporates after deposition. Additionally, the small size of the nanoparticles makes it possible to sinter at much lower temperatures than the bulk material. To prevent aggregation of the particles, ligands or special polymer coatings can be used, which after deposition can be removed with high sintering temperatures [43].

On the other hand, organometallic decomposition inks don't have the risk of agglomeration, can be reduced and sintered at lower temperatures and may lead to lower cost and improved stability [44]. Although most research has focused on silver or copper based organometallic inks, other inks based on metals such as gold, platinum and aluminum have also been reported [45,46].

A variety of different metal-organic complexes have been used to prepare both silver and copper based decomposition inks, aiming to achieve a low-cost ink that can be prepared and sintered at low temperatures and displays good conductivity. A silver-organo-ink formulation proposed by Vaseem et al. [44] uses silver acetate as starting material, and ethylamine and ethanolamine as complexing agents. To ensure effective reduction, the ink was adjusted to pH 10.5 and the resulting silver tracks displayed a conductivity of 2.43×10^7 S/m after applying multiple layers. Another self-reducible ink was made by Shin et al. [37], using copper(II) formate as the starting material and 2-amine-2-methly-1-propanol (AMP) as ligand and n-octylamine as co-complexing agent. After heating the ink to 350 °C the resulting film had a specific resistivity of 9.46 μΩ·cm and was easily transferable using PDMS.

Herein, we propose an ink formulation that incorporates both a silver precursor complex and a copper precursor complex that allows for the simple and fast fabrication of a silver and copper oxide (CuO/Ag) electrode

for H_2O_2 sensing. Upon heating the ink to 150 °C in ambient atmosphere, the ink decomposes and forms particles around 250 nm in size that results in a well connected network. Electrochemical analysis using cyclic voltammetry and amperometry shows that the addition of Cu precursor to the Ag ink resulted in a significant improvement in the electrocatalytic performance. The CuO/Ag electrodes displayed fast response time (< 8s) and a limit of detection of 4.0 μM with a linear range of 5-500 μM. At a working potential of -0.2 V, the sensor experiences little to no interference from other common molecules such as ascorbic acid (AA), glucose (GLU), dopamine (DA) and uric acid (UA). Finally, consecutive measurements showed good reproducibility, repeatability and long-term stability of the electrodes.

2. Experimental

2.1 Reagents

Silver acetate (CH_3CO_2Ag), Copper(II)-formate tetrahydrate (Cuf), 2-Amino-2-methyl-1-propanol, n-Octylamine and ethylamine (C_2H_7N) solution 2M in methanol was purchased from Aldrich. 2-aminoethanol (C_2H_7NO) was purchased from KAN. Formic acid (CH_2O_2), 2-propanol (IPA), Methyl alcohol and hydrogen peroxide (H_2O_2) were purchased from Samchun. Syringe filters were purchased from from Macherey-Nagel. All chemicals and solvents were analytical grade and used without further purification. 0.01M phosphate buffer solutions (PBS) were prepared using phosphate buffered saline tablets from Aldrich.

2.2 Apparatus

Scanning electron microscopy (FESEM, Hitachi S-4800) was used to characterize the morphologies of the electrodes. Thermal gravimetric analysis (TGA) was performed using a TGA/DSC 1 analyzer (Mettler Toledo) with a ramp rate of 10 ºC per minute and keeping a constant temperature at 150 ºC for 15 minutes in air. A Rigaku Smart Lab Diffractometer was used to to obtain the x-ray diffraction (XRD) patterns and X-Ray Photoelectron Spectroscopy (XPS) spectra were obtained using an AXIS-HSi. All electrochemical measurements were performed on an

Autolab potentiostat (Metrohm, USA). A conventional three-electrode system with an Ag/AgCl electrode as reference and platinum wire as counter electrode. The fabricated electrodes were used as working electrode without further treatment. All experiments were performed at room temperature after purging the solution with nitrogen.

2.3 Preparation of Ag and CuO/Ag electrodes

The Ag MOD ink was slightly altered from previous literature [44]. In short, a 2-aminoethanol solution was prepared by mixing 10 ml of C_2H_7NO with 10 ml IPA and then adjusted to pH 10.5 using CH_2O_2. Then, 0.750 ml of the solution was mixed with 0.2 g of CH_3CO_2Ag and 1ml of ethylamine followed by vigorous stirring for 1 minute. Any precipitate was removed using a 0.2 μm syringe filter.

The Cu precursor synthesis was slightly altered from a previously reported method [37]. First 10 mmol 2-Amino-2-methyl-1-propanol, 10 mmol of n-Octylamine and 5 mL of Methyl alcohol were mixed in a 500ml round bottom flask and stirred for 10 min. Then 10 mmol of copper(II) formate tetrahydrate was added to the mixture and sonicated for 30 min to form a homogeneous Cuf-AMP-Octylamine complexes. The methyl alcohol and water were then evaporated under reduced pressure at 60 ºC. The obtained Cuf-AMP-Octylamine complex had a dark-blue color and was diluted with 1.5 g IPA to lower the viscosity.

The Ag MOD ink and the Cu precursor were mixed in an 85 to 15 volume ratio and 50 µl was drop cast on a 1.5 cm by 4 cm polyimide film. The film was heated on a hotplate at 150 ºC in air for 30 minutes. After cooling down to room temperature, epoxy was used to define a 1 cm^2 working area.

3. Results and Discussion

3.1 Characterization of the Ag and CuO/Ag electrodes

The synthesis of the Ag ink and Cu precursor closely followed previously reported methods [37,44]. To prevent any precipitation upon addition of the Cu precursor to the Ag ink, the solvent of the ink was replaced by IPA and the Ag loading was decreased. The thermal decomposition of the Cu-Ag ink was investigated using thermogravimetric analysis (TGA) and shown in Fig. 1. There was a continuous weight loss starting at room temperature up to 150 ºC. The graph displays a clear two-step weight loss. The first step was completed around 50 ºC and corresponds with the evaporations of low boiling point solvents. The second step from 50 to 150 ºC corresponds to the decomposition of both the silver and copper complexes. A negligible weight loss was observed at temperatures above 150 ºC, indicating that both complexes were fully decomposed.

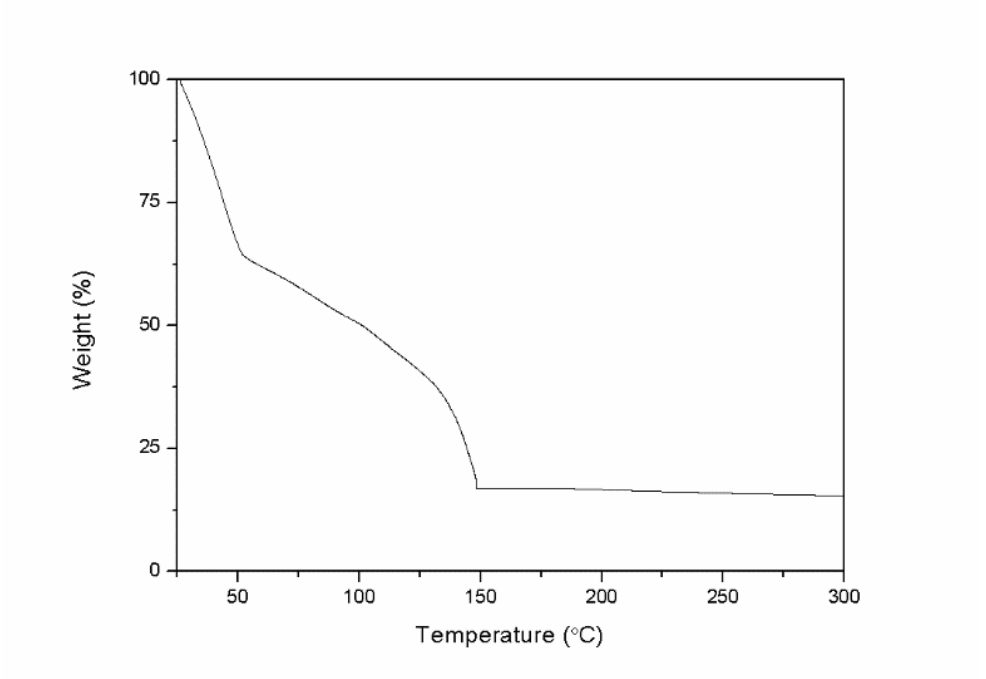

Figure 1. TGA of the hybrid ink containing both Ag and Cu precursor complexes in air.

When heated the reduction of Ag ions in the Ag ink could clearly be observed by a color change from transparent, to black, followed by white. The hybrid ink containing both Ag and Cu turned from blue to black, to a yellow-grey color as shown in Fig. 2A. Heating ink formulations with higher Cu concentration resulted in a darker yellow-black colored films.

The morphology and structural details of the Ag and CuO/Ag electrodes were investigated by SEM. The hybrid ink forms a film with a thickness of several μm on top of the polyimide substrate, shown in Fig. 2B. Furthermore, Fig. 2C shows that the sintered Ag particles are relatively polydisperse and form a connective three-dimensional network. The majority of the particles are in the 200-300 nm range with a few outliers that are considerably bigger in size. The CuO/Ag electrode (Fig. 2D) has a similar morphology with most particles around 200-300 nm range but the particles appear less distinct and more connected. This difference can possibly be explained by the formation mechanism; the ligands used to stabilize the silver ions decompose and evaporate at a lower temperature than the ligands around the copper ions, resulting in the formation of silver particles followed by the reduction of copper ions on the already existing silver network.

The EDS spectrum (Fig. 2H) clearly shows the presence of both Cu and O in the composite film, suggesting that Cu was indeed present in its oxidized form. Furthermore, the EDS elemental mapping of Ag, Cu and O

indicates that CuO was homogeneously distributed throughout the Ag network and the EDS spectra showed a molar ratio between Ag and Cu of 74.7 to 25.3. Inductively coupled plasma optical emission spectroscopy (ICP-OES) was used to accurately determine the presence of Ag and Cu in the composite material and the results show a molar ratio of 76 to 24 between Ag and Cu, which is in close agreement with the theoretically calculated ratio of 76.3 to 23.7, as shown in Table 1.

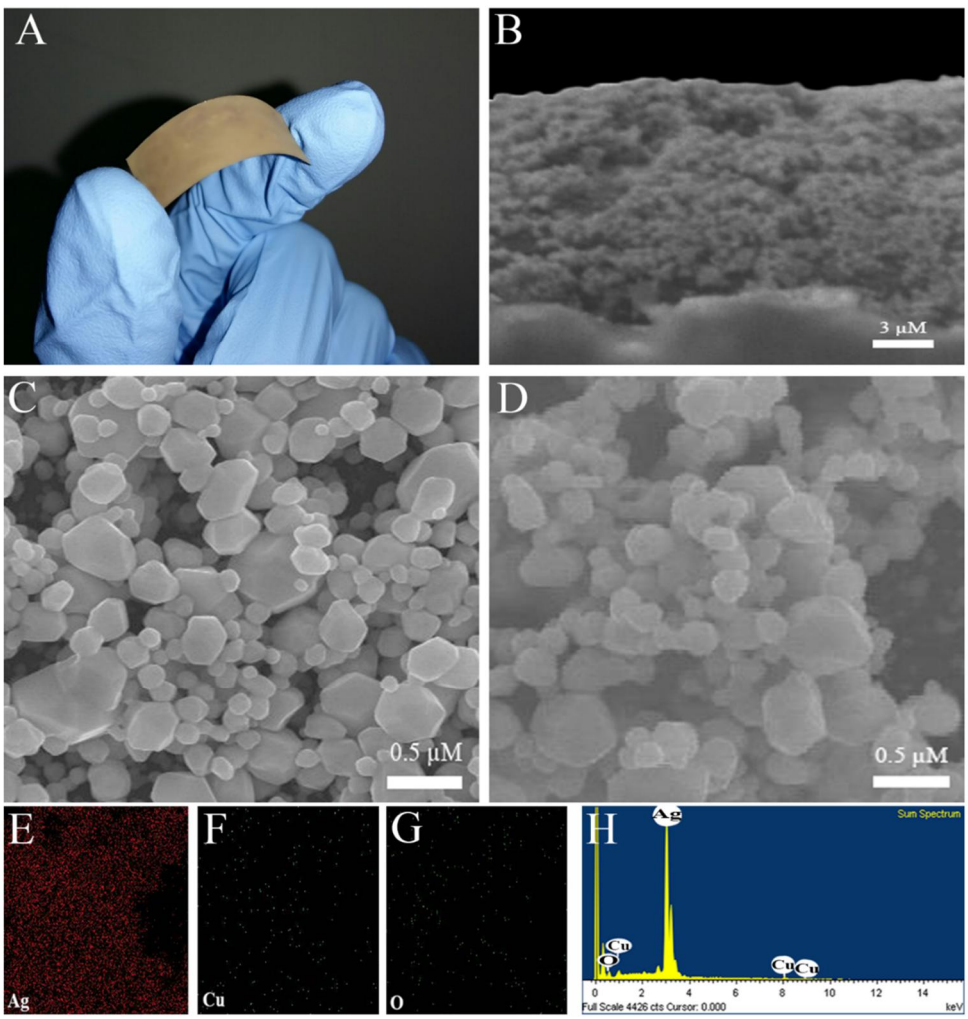

Figure 2. Optical image of the fabricated sensor (A), SEM images of the Ag (C) and CuO/Ag (D) electrodes including a cross-sectional image of the CuO/Ag film (B), and EDS mapping and spectrum of the CuO/Ag electrode (E-H).

Element	Calculated	EDS	ICP-OES
Ag	76,3 %	74,7 %	76,0 %
Cu	23,7 %	25,3 %	24,0 %

Table 1 Comparison of the calculated and measured molar ratio between Ag and Cu of the CuO/Ag electrode.

Additionally, XRD was used to further examine the chemical composition of the CuO/Ag electrode and the results are shown in Fig. 3A. Clear diffraction peaks were observed at 38.18º, 44.36º, 64.58º and 77.59º, which can be indexed as the {1 1 1}, {2 0 0}, {2 2 0} and {3 1 1} planes of Ag respectively (JCPDS no. 87-0720). No clear diffraction peaks that correspond with CuO were observed. This could be because CuO is only formed at the surface of the film where the ink is in contact with the oxygen containing atmosphere. The copper ions that were not located at the air-liquid interface during heating could possibly have formed an Ag-Cu bimetallic structure. Therefore, the absence of copper related peaks could be explained by the relatively low concentration of CuO in the overall film and the difficulty of obtaining clear XRD peaks for Ag-Cu bimetallic nanoparticle as reported by several other papers [47–51]. However, the presence of CuO on the surface of our film is confirmed by the Ag 3d and Cu 2p XPS spectra of the CuO/Ag electrode, as shown in Fig. 3B and Fig. 3C. The peaks at 368.8 eV and 374.8 eV corresponds with the binding energies of Ag 3d5/2 and Ag 3d3/2 of metallic Ag^0 respectively [52,53]. In contrast to the XRD data, the XPS spectrum shows two peaks at 933.9 eV and 953.8 eV which corresponds to the binding energies of Cu 2p3/2 and Cu 2p1/2, clearly indicating the presence of Cu in the sample. Additionally, the shake-up satellite peaks at 944.8 eV and 963.5 eV suggests that the copper is in the form of Cu^{2+} [54,55].

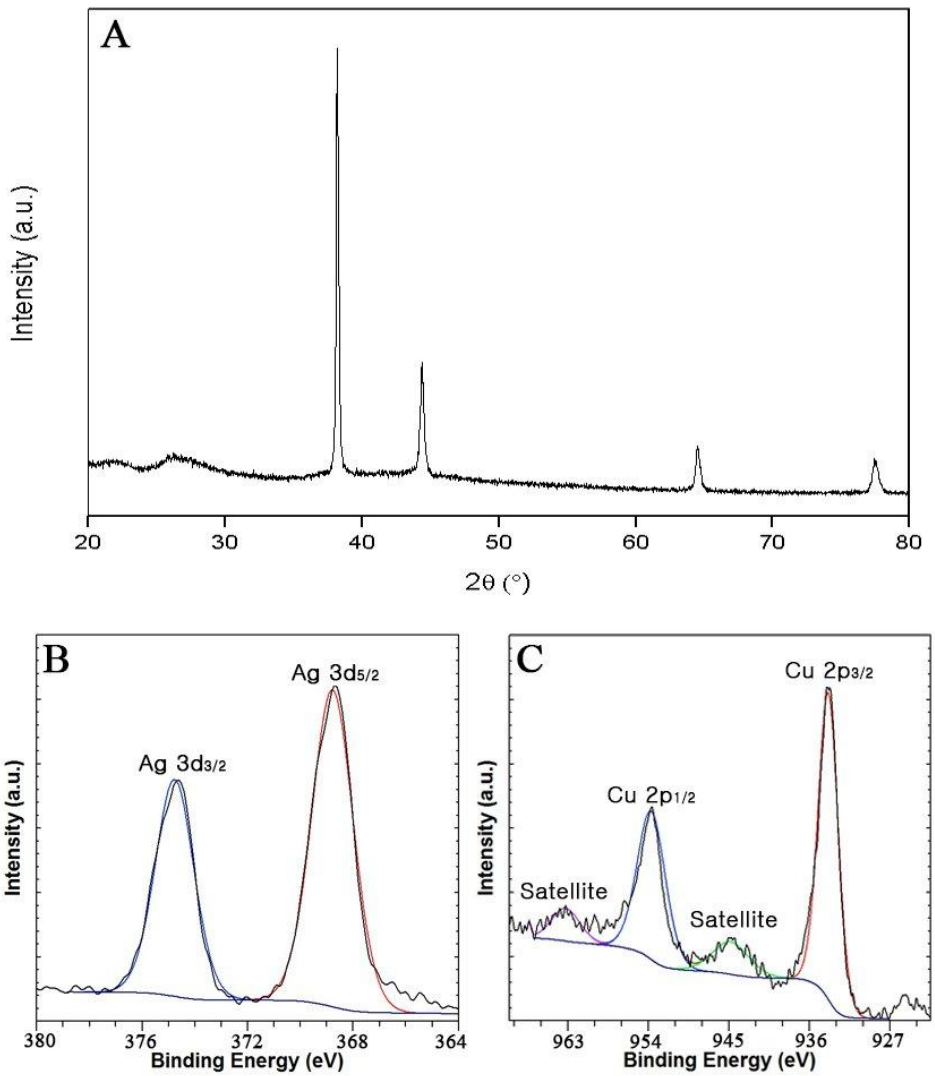

Figure 3. XRD patterns of the CuO/Ag nanocomposite electrode (A) and the XPS spectra of the Ag 3d (B) and Cu 2p regions (C).

3.2 Electrochemical characterization of the Ag and CuO/Ag electrodes

Fig. 4 shows the cyclic voltammograms of the Ag and CuO/Ag electrodes in the absence and presence of 1 mM of H_2O_2. In absence of H_2O_2, the Ag electrode shows no electrochemical response. In contrast, the CuO/Ag electrode exhibits a clear redox couple in between 0 V and -0.2 V, which can be attributed to the oxidation of Cu_2O to CuO and vice versa [28]. After addition of 1 mM H_2O_2 both Ag and CuO/Ag electrode show a distinct peak at -0.49 V due to the electrochemical reduction of H_2O_2 on Ag. The mechanism of H_2O_2 reduction on the Ag is given as:

$$H_2O_2 + e^- \rightarrow OH_{(ads)} + OH^- \quad (1)$$

$$H_2O_2 + H^+ + OH_{(ads)} + e^- \rightarrow 2OH_{(ads)} + H_2O \quad (2)$$

The significant increase of peak current of the CuO/Ag electrode compared to the Ag electrode suggests that the small addition of copper to the Ag ink increases the overall conductivity of the sensor [32]. Furthermore, the addition of a small amount of CuO can slightly alter the electronic structure and affect the $OH_{(ads)}$ rate, improving the composites electrochemical performance.

Moreover, for the CuO/Ag electrode the peak corresponding to the reduction of CuO to Cu_2O shift to a more negative potential of -0.36 V. The considerable increased in reduction peak current and the small increase of the oxidation peak current of the Cu redox couple after addition of H_2O_2

indicates the indirect electrochemical reduction of H_2O_2 on the copper oxide surface, according to the previously reported mechanism [56]:

$$Cu_2O + H_2O_2 \rightarrow 2\ CuO + H_2O \quad (3)$$

$$2\ CuO + H_2O + 2e^- \rightarrow Cu_2O + 2OH^- \quad (4)$$

The catalytic activity of the CuO/Ag electrode was further studied by changing the concentration of H_2O_2 ranging from 0 to 3 mM as shown in Fig. 5. The gradual increase of peak current with increasing concentration of H_2O_2 indicates good performance towards H_2O_2 reduction.

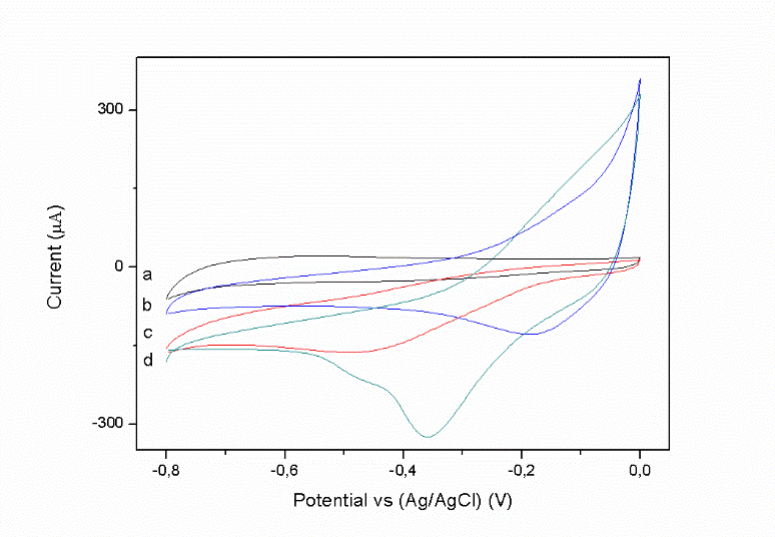

Figure 4. Cyclic voltammograms of Ag and CuO/Ag electrodes in absence (a,b) and presence of 1 mM H_2O_2 (c,d) in PBS (pH 7.4) at a scan rate of 0.05 V s^{-1}.

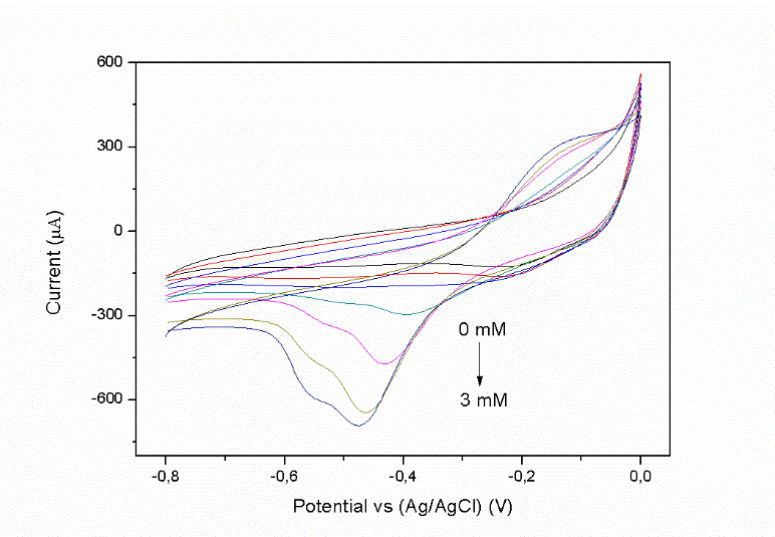

Figure 5. Cyclic voltammograms of CuO/Ag with successive additions of 0.5 mM H_2O_2 in PBS (pH 7.4) at a scan rate of 0.05 V s^{-1}.

To investigate the possible kinetic mechanism the influence of scan rate on the voltammetric response of H_2O_2 reduction was studied and shown in Fig. 6. A slight shift of peak potentials to more positive values at higher scan rate was observed. The inset shows the linear relationship between the reduction peak current and the square root of the scan rate, indicating that the reduction of H_2O_2 at the CuO/Ag electrode surface is diffusion-controlled [57].

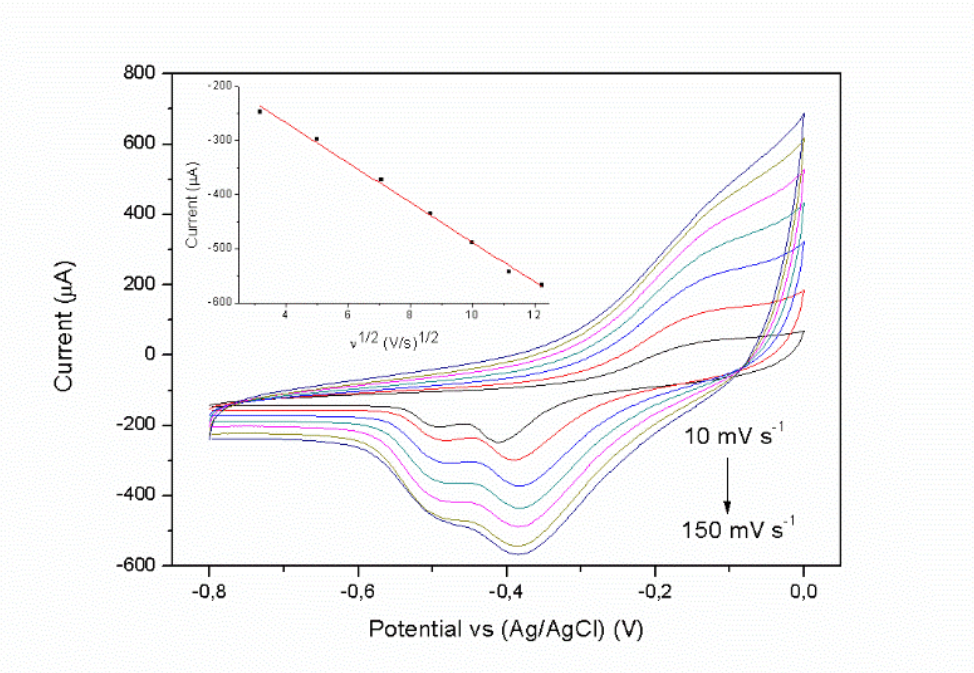

Figure 6. Cyclic voltammograms of CuO/Ag at different scan rates in 1 mM H_2O_2 in PBS (pH 7.4) at 10, 25, 50, 75, 100, 125, 150 mV s^{-1}. Inset: plot of the peak current vs. square root of scan rates.

Fig. 7 shows the amperometric current-time response upon sequential addition of different concentrations of H_2O_2. Every 50 seconds an amount of H_2O_2 was added ranging from 5 μM to 50 μM. The sensor showed a fast response time and reached 75% and 95% of the steady state current within 8 and 16 seconds respectively. The inset shows a linear relation between the steady state reduction current and the concentration of H_2O_2 with a linear range of 50-500 μM and a correlation coefficient of 0.997. The detection limit was calculated to be 4.0 μM with a signal to noise ratio of S/N=3. A comparison of our CuO/Ag electrode with other previously reported non-enzymatic sensors based on Ag, CuO or Cu_2O is given in Table 2. In terms of limit of detection, our sensor is comparable with other values mentioned before in literature.

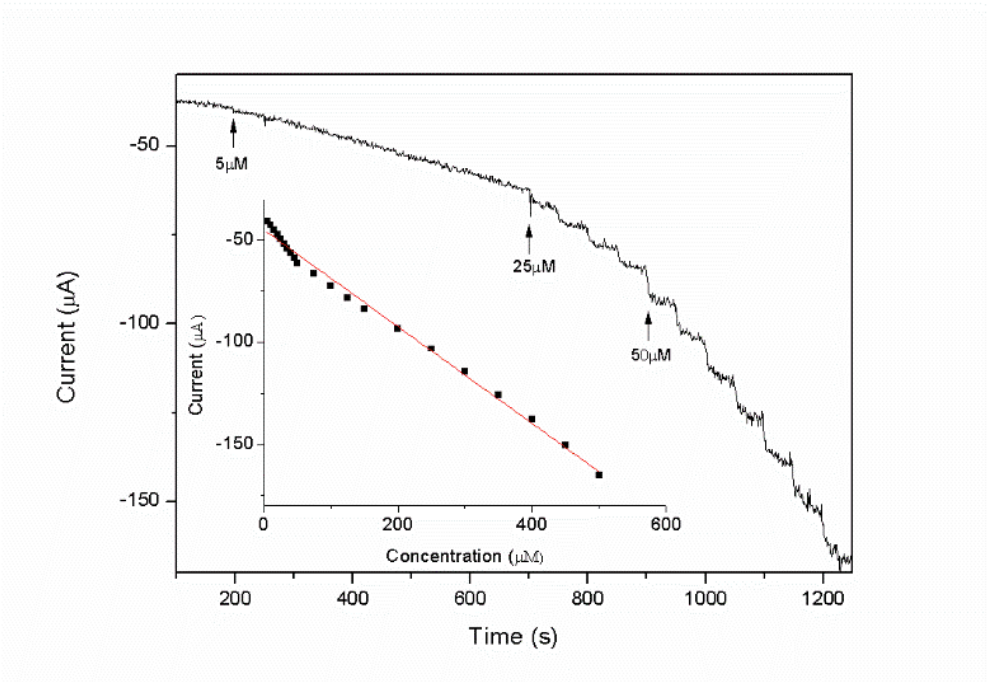

Figure 7. Chronoamperometric response of CuO/Ag upon successive additions of H_2O_2 into PBS (pH 7.4) while stirring, applied potential: -0.2 V. Inset: correlation between different H_2O_2 concentrations and current.

Electrode Material	Limit of Detection (μM)	References
Porous Ag	29.8	[58]
Ag Microspheres	1.2	[59]
Ag Nanowires	29.2	[60]
Ag Nanoparticles	1.0	[61]
Cu_2O Cube/ Graphene Nanosheet	20.8	[28]
CuO Nanorod Bundles	0.22	[62]
CuO Nanoflowers	0.167	[63]
Ag/Cu_2O Cubes	0.7	[39]
CuO/Ag Composite	4.0	This Work

Table 2. Comparison of the performance of non-enzymatic sensors based on Ag, CuO or Cu_2O for the detection of H_2O_2.

The effect of the Cu precursor volume ratio in the ink was investigated by mixing the Ag MOD ink and the Cu precursor in different volume ratios and testing the LOD of the resulting electrodes. Fig. 8 shows that the Ag electrode had a limit of detection of 20 μM and adding a small amount of Cu lowers the limit of detection with an optimum of 4.0 μM at a Cu concentration of 23.7%. Further increasing the Cu precursor content drastically increased the resistivity of the film, and the resulting electrodes could not be used as a sensor.

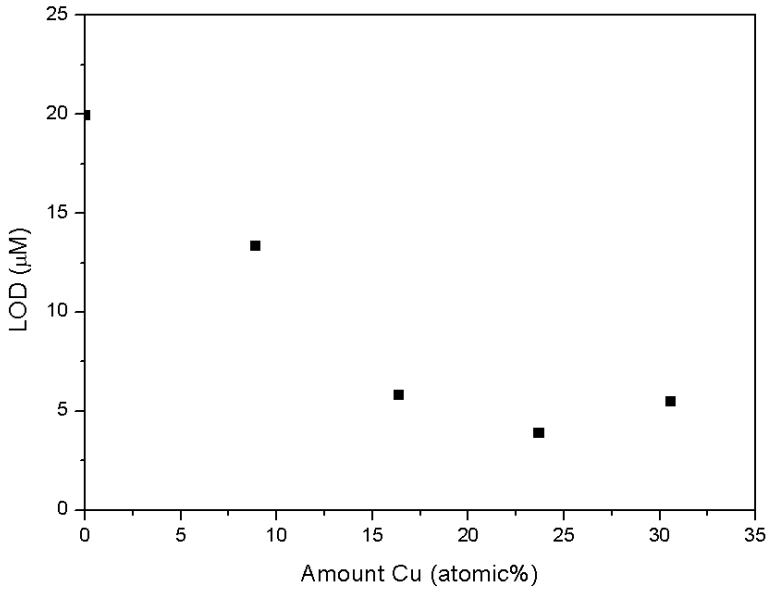

Figure 8. Relation between between the obtained limit of detection and the amount of Cu present in the CuO/Ag electrode.

To examine the selectivity of the CuO/Ag electrode, a small interference test was conducted. The response to 0.2 mM of H_2O_2 at a potential of -0.2 V was compared to the addition of 0.2 mM of ascorbic acid (AA), glucose (GLU), dopamine (DA) and uric acid (UA), which are other commonly found electroactive compounds [64,65]. As shown in Fig. 9, a big current change was observed upon addition of H_2O_2, while the addition of AA, GLU, DA or UA had no significant effect. This result suggests that the CuO/Ag electrode has good selectivity towards H_2O_2.

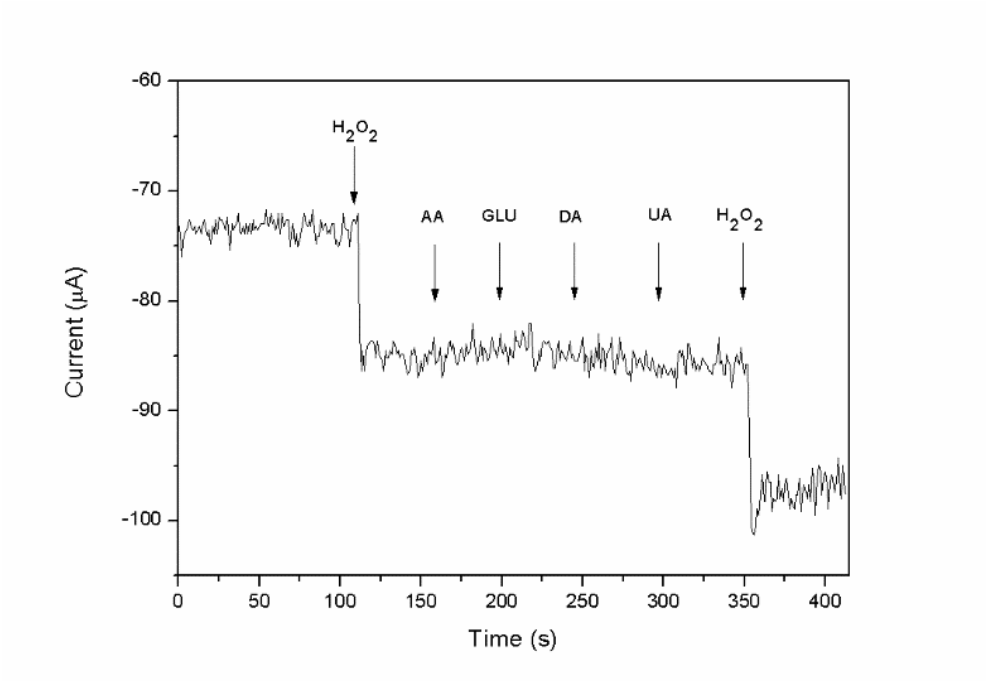

Figure 9. Chronoamperometric response of the CuO/Ag sensor upon addition of H_2O_2 and common interfering substances into PBS (pH 7.4) while stirring, applied potential: −0.2 V.

3.3 Reproducibility and stability

Five additional CuO/Ag electrodes were prepared using the same method and used to measure H_2O_2 under the same conditions. The measured limit of detection of H_2O_2 among the five electrodes had a standard deviation of less than 0.5 μM and a relative standard deviation (RSD) of 11%, as shown in Table 3. Additionally, the amperometric response to 7 consecutive additions of 5 μM H_2O_2 using the same electrode was measured and the RSD was determined to be less than 7%, as shown in Table 4. To test the long-term stability, the sensor was stored in air at 4 ºC. After 2 weeks, the amperometric response to the addition of 5 μM and 50 μM showed no significant decreased in current.

Sample	Limit of Detection (µM)
1	3,91
2	3,56
3	3,93
4	4,10
5	4,74
Mean	4,05
Standard Deviation	0,43

Table 3 The measured limit of detection of 5 different CuO/Ag electrode sample.

Amount of H_2O_2 (µM)	Current Change (µA)
5	2,40
5	2,15
5	2,41
5	2,24
5	2,44
5	2,32
5	2,61
Mean	2,37
Standard Deviation	0,15

Table 4 Current response of the CuO/Ag electrode to 7 consecutive additions of 5 µM H_2O_2.

4. Conclusions

In summary, a novel formulation for a hybrid precursor ink was proposed and used to fabricate a CuO/Ag composite material film. The hybrid ink can be fully decomposed at low temperatures and in the resulting structure, CuO forms on top of the conductive Ag network. Both Ag and CuO/Ag electrodes were used to make an amperometric sensor for the detection of H_2O_2. After optimizing the ratio between CuO and Ag the composite showed a significantly lower limit of detection than the pure Ag electrode. The synergistic effects between Ag and CuO and the improved connectivity between particles can possibly explain the enhanced sensing performance of the composite material over pure Ag. Furthermore, the hybrid ink method can possibly be extended to a generalized approach for synthesizing other silver-based composite materials. This work shows promising preliminary results for further research into the application of hybrid inks for electrochemical sensing and similar applications.

References

[1] M. Giorgio, M. Trinei, E. Migliaccio, and P. G. Pelicci, Nat. Rev. Mol. Cell Biol. **8**, 722 (2007).

[2] F. Wang, R. Han, G. Liu, H. Chen, T. Ren, H. Yang, and Y. Wen, J. Electroanal. Chem. **706**, 102 (2013).

[3] W. Chen, S. Cai, Q.-Q. Ren, W. Wen, and Y.-D. Zhao, Analyst **137**, 49 (2012).

[4] P. N. Bartlett, P. R. Birkin, J. H. Wang, F. Palmisano, and G. De Benedetto, Anal. Chem. **70**, 3685 (1998).

[5] E. C. Hurdis and H. Romeyn Jr, Anal. Chem. **26**, 320 (1954).

[6] N. V Klassen, D. Marchington, and H. C. E. McGowan, Anal. Chem. **66**, 2921 (1994).

[7] R. M. Sellers, Analyst **105**, 950 (1980).

[8] C. Matsubara, N. Kawamoto, and K. Takamura, Analyst **117**, 1781 (1992).

[9] Y. B. Tsaplev, J. Anal. Chem. **67**, 506 (2012).

[10] S. Hanaoka, J.-M. Lin, and M. Yamada, Anal. Chim. Acta **426**, 57 (2001).

[11] J. Hong, J. Maguhn, D. Freitag, and A. Kettrup, Fresenius. J. Anal. Chem. **361**, 124 (1998).

[12] F. Wen, Y. Dong, L. Feng, S. Wang, S. Zhang, and X. Zhang, Anal. Chem. **83**, 1193 (2011).

[13] S. Xiaohong, C. Ying, Y. Hongyan, G. Shangfeng, and X. Dan, Anal. Chem. **79**, 3695 (2007).

[14] W. Zhao, H. Wang, X. Qin, X. Wang, Z. Zhao, Z. Miao, L. Chen, M. Shan,

Y. Fang, and Q. Chen, Talanta **80**, 1029 (2009).

[15] Y. Li, J. Zhang, H. Zhu, F. Yang, and X. Yang, Electrochim. Acta **55**, 5123 (2010).

[16] L. Wang and E. Wang, Electrochem. Commun. **6**, 225 (2004).

[17] A. Uzunoglu, S. Song, and L. A. Stanciu, J. Electrochem. Soc. **163**, B379 (2016).

[18] S. Chen, R. Yuan, Y. Chai, and F. Hu, Microchim. Acta **180**, 15 (2013).

[19] A. Gutes, I. Laboriante, C. Carraro, and R. Maboudian, Sensors Actuators B Chem. **147**, 681 (2010).

[20] X. Li, X. Liu, W. Wang, L. Li, and X. Lu, Biosens. Bioelectron. **59**, 221 (2014).

[21] X. J. Wang, X. L. Wan, and J. R. Wang, Cryst. Res. Technol. **49**, 474 (2014).

[22] W. Liu, H. Zhang, B. Yang, Z. Li, L. Lei, and X. Zhang, J. Electroanal. Chem. **749**, 62 (2015).

[23] C. Karuppiah, S. Palanisamy, S.-M. Chen, V. Veeramani, and P. Periakaruppan, Sensors Actuators B Chem. **196**, 450 (2014).

[24] X. Liu, H. Zhu, and X. Yang, Talanta **87**, 243 (2011).

[25] Y. Zhang, Z. Wang, Y. Ji, S. Liu, and T. Zhang, RSC Adv. **5**, 39037 (2015).

[26] Z. Yang, X. Zheng, and J. Zheng, RSC Adv. **6**, 58329 (2016).

[27] W. Lu, F. Liao, Y. Luo, G. Chang, and X. Sun, Electrochim. Acta **56**, 2295 (2011).

[28] M. Liu, R. Liu, and W. Chen, Biosens. Bioelectron. **45**, 206 (2013).

[29] Y. Li, Y. Zhang, Y. Zhong, and S. Li, Appl. Surf. Sci. **347**, 428 (2015).

[30] Z. Li, X. Zheng, and J. Zheng, New J. Chem. **40**, 2115 (2016).

[31] X. Li, L. Wang, Q. Wu, Z. Chen, and X. Lin, J. Electroanal. Chem. **735**, 19 (2014).

[32] J. S. Easow and T. Selvaraju, Electrochim. Acta **112**, 648 (2013).

[33] S. Dong, Q. Yang, L. Peng, Y. Fang, and T. Huang, Sensors Actuators B Chem. **232**, 375 (2016).

[34] H. Li, C.-Y. Guo, and C.-L. Xu, Biosens. Bioelectron. **63**, 339 (2015).

[35] S. E. Jeena, P. Gnanaprakasam, A. Dakshinamurthy, and T. Selvaraju, RSC Adv. **5**, 48236 (2015).

[36] L. Rahman, A. Shah, S. K. Lunsford, C. Han, M. N. Nadagouda, E. Sahle-Demessie, R. Qureshi, M. S. Khan, H.-B. Kraatz, and D. D. Dionysiou, RSC Adv. **5**, 44427 (2015).

[37] D.-H. Shin, S. Woo, H. Yem, M. Cha, S. Cho, M. Kang, S. Jeong, Y. Kim, K. Kang, and Y. Piao, ACS Appl. Mater. Interfaces **6**, 3312 (2014).

[38] M. Vaseem, S.-K. Lee, J.-G. Kim, and Y.-B. Hahn, Chem. Eng. J. **306**, 796 (2016).

[39] C. Qi and J. Zheng, Electroanalysis **28**, 477 (2016).

[40] D. Li, L. Meng, S. Dang, D. Jiang, and W. Shi, J. Alloys Compd. **690**, 1 (2017).

[41] L. Huang, Y. Huang, J. Liang, X. Wan, and Y. Chen, Nano Res. **4**, 675 (2011).

[42] Y. Dong, X. Li, S. Liu, Q. Zhu, M. Zhang, J.-G. Li, and X. Sun, Thin Solid Films **616**, 635 (2016).

[43] J. Perelaer, P. J. Smith, D. Mager, D. Soltman, S. K. Volkman, V.

Subramanian, J. G. Korvink, and U. S. Schubert, J. Mater. Chem. **20**, 8446 (2010).

[44] M. Vaseem, G. McKerricher, and A. Shamim, ACS Appl. Mater. Interfaces **8**, 177 (2015).

[45] H. M. Nur, J. H. Song, J. R. G. Evans, and M. J. Edirisinghe, J. Mater. Sci. Mater. Electron. **13**, 213 (2002).

[46] C. Curtis, A. Miedaner, M. van Hest, and D. Ginley, WO/2009/059273 (2010).

[47] J. Yun, K. Cho, B. Park, H. C. Kang, B. K. Ju, and S. Kim, Jpn. J. Appl. Phys. **47**, 5070 (2008).

[48] M. Taner, N. Sayar, I. G. Yulug, and S. Suzer, J. Mater. Chem. **21**, 13150 (2011).

[49] C.-H. Huang, H. P. Wang, J.-E. Chang, and E. M. Eyring, Chem. Commun. **2**, 4663 (2009).

[50] S. Delsante, G. Borzone, R. Novakovic, D. Piazza, G. Pigozzi, J. Janczak-Rusch, M. Pilloni, and G. Ennas, Phys. Chem. Chem. Phys. **17**, 28387 (2015).

[51] C. K. Kim, G.-J. Lee, M. K. Lee, and C. K. Rhee, Powder Technol. **263**, 1 (2014).

[52] M. Pang, J. Hu, and H. C. Zeng, J. Am. Chem. Soc. **132**, 10771 (2010).

[53] V. Djoković, R. Krsmanović, D. K. Božanić, M. McPherson, G. Van Tendeloo, P. S. Nair, M. K. Georges, and T. Radhakrishnan, Colloids Surf. B **73**, 30 (2009).

[54] M. Kuang, T. Tao Li, H. Chen, S. Mao Zhang, L. Li Zhang, and Y. Xin

Zhang, Nanotechnology **26**, 304002 (2015).

[55] J. S. Shaikh, R. C. Pawar, A. V. Moholkar, J. H. Kim, and P. S. Patil, Appl. Surf. Sci. **257**, 4389 (2011).

[56] M. V Vazquez, S. R. De Sanchez, E. J. Calvo, and D. J. Schiffrin, J. Electroanal. Chem. **374**, 179 (1994).

[57] J. F. Rusling and A. E. F. Nassar, J. Am. Chem. Soc. **115**, 11891 (1993).

[58] E. Kurowska-Tabor, K. Gawlak, K. Hnida, M. Jaskuła, and G. D. Sulka, Electrochim. Acta **213**, 811 (2016).

[59] B. Zhao, Z. Liu, Z. Liu, G. Liu, Z. Li, J. Wang, and X. Dong, Electrochem. Commun. **11**, 1707 (2009).

[60] E. Kurowska, A. Brzózka, M. Jarosz, G. D. Sulka, and M. Jaskuła, Electrochim. Acta **104**, 439 (2013).

[61] C. M. Welch, C. E. Banks, A. O. Simm, and R. G. Compton, Anal. Bioanal. Chem. **382**, 12 (2005).

[62] C. Batchelor-McAuley, Y. Du, G. G. Wildgoose, and R. G. Compton, Sensors Actuators B Chem. **135**, 230 (2008).

[63] M.-J. Song, S. W. Hwang, and D. Whang, Talanta **80**, 1648 (2010).

[64] Z. Li, X. Zheng, Q. Sheng, Z. Yang, and J. Zheng, RSC Adv. **6**, 11218 (2016).

[65] S. Zhang, L. Han, C. Hou, C. Li, Q. Lang, L. Han, and A. Liu, J. Electroanal. Chem. **742**, 84 (2015).

국문초록

과산화 수소는 다양한 생물학적 반응에 필수적일 뿐만 아니라 산업분야에서도 가지각색 역할을 한다. 과산화 수소의 역할로는 산화제로서 종이를 표백하는 것과 소독제로서 폐수처리를 하는 것 등이 있다. 과산화 수소가 다양한 분야에서 사용하고 있으나 잔류 농도가 75 ppm 보다 높으면 건강에 해롭고 암을 유발할 수 있다. 기존의 과산화 수소 검출과 분석방법으로는 역가측정법 (titration), 분광광도법 (spectrophotometry), 화학 발광법 (chemiluminescence)등이 있다. 하지만 이러한 방법들은 비용이 높거나 복잡하다는 단점이 있어 전기화학에 기반을 둔 검출이 선호된다. 기존에 많이 연구되었던 효소 기반 전기화학 센서는 민감하나 불안정하고 복잡한 합성이 요구되기 때문에 연구가 지체되고 있는 반면에 금이나 은과 같은 나노입자로 제작된 센서는 안정하고 저렴하여 각광받고 있다. 본 연구에서는 과산화 수소

검출을 위해 저렴하고 간편한 제조방법을 이용한 전기화학 센서를 개발하였다. 이 센서 전극의 제조는 은과 구리 전구체 잉크 혼합물을 환원분위기나 고온이 아닌 대기 하에서 저온소결을 통해 진행된다. 잉크 분해 과정은 TGA 를 통해 분석하였으며, 입자의 크기와 형태는 HR-TEM, EDS 를 통해 밝혔다. TGA 결과를 통해 150 °C 에서 잉크가 완전히 분해되는 것을 확인했으며 완전 소결 뒤에 250 nm 크기의 나노입자로 구성된 네트워크 형태를 전자현미경으로 확인 하였다. 또한 전기화학 분석에 따르면 선형 응답 범위는 50 ~ 500 μM 이었고 검출한계는 4.0 μM 이었다. 순수한 은 잉크로 제작된 전극과 비교하여 은과 구리로 합성된 전극의 우월한 성능을 확인하였다.

주요어: **산화동-은 구조체, 전구체 잉크, 비효소적 센서, 과산화 수소**

학 번: **2015-26112**